

Dynamics of the Amorphous and Crystalline α -, γ -Phases of Indomethacin

L. Carpentier,* R. Decressain, S. Desprez, and M. Descamps

Laboratoire de Dynamique et Structure des Matériaux Moléculaires, U.M.R. CNRS 8024,
Bât. P5, Ust Lille, 59655 Villeneuve d'Ascq, France

Received: June 29, 2005; In Final Form: October 19, 2005

Crystallization processes in indomethacin can be observed below T_g leading to different forms depending on the thermal treatment: a rapid and deep quench below T_g leads to the metastable α -phase and a slow cooling close to T_g gives rise to the stable γ -phase. To understand this atypical behavior, we have studied the molecular mobility of the amorphous and crystalline forms of indomethacin by dielectric relaxation and ^1H NMR spectroscopy. Two relaxations were detected in the glassy state obtained from the deeply quenched liquid. One, also present in the γ -phase, was attributed to local rotations. The other one, of very low amplitude, was attributed to the Johari–Goldstein relaxation. The results allowed to discuss the relationship between these two relaxation processes and the crystallization properties of amorphous indomethacin.

I. Introduction

The problem of the stability of amorphous and crystalline forms is a fundamental concern to pharmaceutical and food scientists.^{1,2} Although the more stable crystalline forms favor the manufacturing and conservation of drugs, the amorphous form offers the possibility to improve dissolution rates and bioavailability. The underlying tendency of amorphous pharmaceutical materials to crystallize needs to be controlled through the selection of adequate processing and storage conditions. The solid state crystallization is generally thought to be restricted to the temperature domain located above the glass transition temperature T_g , below T_g any diffusional transport process required for nucleation and crystal growth being inhibited. However, there are a lot of experimental evidences of crystallization observed below T_g .³ It has been suggested that such a process can be related to the subsistence of a nonnegligible mobility. In many small molecular weight organic compounds the viscosity at T_g is 2–3 orders of magnitude lower than the commonly expected value $\eta = 10^{13}$ P.⁴ As a possible other origin, the dynamic effects controlling the nucleation and growth in the amorphous state can be related to the rotational diffusion rather than to the translational diffusion. It seems reasonable to assume that such rotational diffusion can favor the formation of nuclei between the nearest neighbors.

The knowledge of the dynamic properties which mainly drive the kinetics of transformation between the different forms is a fundamental aspect of the preservation of materials. As a model pharmaceutical substance, indomethacin is of particular interest. It exhibits a polymorphism that manifests differently depending on the thermal history and the previous vitrification.^{5,6} The dynamics of the amorphous form has been characterized over a wide range of times and temperatures using several experimental techniques: dielectric relaxation,⁷ viscosity,⁸ calorimetric measurements,⁹ and thermally stimulated depolarized current (TSDC).¹⁰ Concerning this latter study, the data have strongly suggested the existence of an additional relaxation process below

T_g . To enlighten this problem, we have performed additional dielectric measurements, which are confronted with ^1H NMR analyses. In particular, the differences of molecular mobility depending on the preparation conditions and their influence on the crystallization are analyzed. To determine the origin of the secondary relaxation, we also studied the dynamic properties of the two main crystalline forms, the α - and γ -phase. Their confrontations aimed to search for the origin of the crystallization processes taking place in a temperature domain where the mobility is intrinsically reduced.

II. Materials and Methods

II.1. Physical States of Indomethacin: An Overview. Indomethacin (Figure 1) $\text{C}_{19}\text{H}_{16}\text{ClNO}_4$ (1-(*p*-chlorobenzoyl)-5-methoxy-2-methylindole-3-acetic acid) is a nonhygroscopic compound in its crystalline form exhibiting at least two polymorphic varieties¹¹ of known crystalline structure afterward called α and γ . These two phases constitute a monotropic system whose more stable form at room temperature is the γ -phase which melts at $T_m = 434$ K.⁶ The thermal properties of the three forms studied in this paper are summarized in Table 1. The slowly cooled liquid showed no tendency to crystallization over a period of up to 2 years at room temperature.¹² However, once the amorphous sample is triturated and held close to or below its glass transition temperature, crystallization of the γ -phase can occur over a long period while crystallization at higher temperature favors the formation of the α -phase.⁵ The same transformations can also be observed upon heating or during isothermal conditions, after a rapid and deep quench of amorphous indomethacin at the liquid nitrogen temperature.⁶

Crystal of γ -indomethacin belongs to the centrosymmetric triclinic space group $\text{P}\bar{1}$ with $Z = 2$.¹³ The crystal packing is dominated by the hydrogen bonding of the carboxylic acid group to form molecular dimers. The crystal structure of the α -phase belongs to the monoclinic space group $\text{P}2_1$ with 3 molecules in the asymmetric unit, adopting 3 very different conformations as compared to the single conformation in the γ -phase. The resulting organization in trimers of the α -phase is supposed to be at the origin of its higher density.¹⁴ All these characteristics are summarized in Table 2.

* Corresponding author. E-mail: laurent.carpentier@univ-lille1.fr.
Telephone: (+33) 3 20 43 68 34.

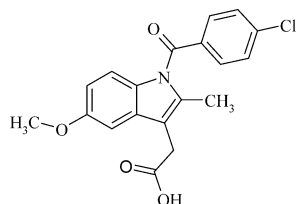


Figure 1. Molecular structure of indomethacin.

TABLE 1: Thermal Characteristics of the Amorphous and Polymorphic Forms of Indomethacin

α -phase	γ -phase	amorphous form
$T_{m\alpha} = 428$ K	$T_{m\gamma} = 434$ K	T_g (2 K/min) = 315 K
$H_{m\alpha} = 91$ J g ⁻¹	$H_{m\gamma} = 110$ J g ⁻¹	$\Delta C_p(T_g) = 0.466$ J g ⁻¹ K ⁻¹

TABLE 2: Structural Characteristics of the Polymorphic Forms of Indomethacin

	space group	Z	density (g cm ⁻³)
α -phase ¹⁴	$P2_1$	6	1.40
γ -phase ¹³	$P1$	2	1.38

II.2. Experimental Procedures. Samples Preparation. A highly pure crystalline powder (99.9%) was obtained from Aldrich Chemical Co. in the crystalline γ -phase and used as received. The α -phase was obtained by dissolution in methanol and precipitation in water as described in ref 15. Amorphous indomethacin was prepared by melting the γ -phase at 440 K.

Dielectric Relaxation. The dielectric measurements were performed with the analyzer DEA 2970 of TA Instrument which provides nearly 7 decades of frequency (3 mHz – 100 kHz), thus facilitating a complete assessment of glass behavior (the kinetic criterion usually fixes the characteristic frequency ν (T_g) \approx 10 mHz). The dielectric cell consists of an interdigitated array of electrodes on which the sample was melted, allowing an optimal filling of the cell. This thermal processing is greatly facilitated by the ability of the compound to resist against parasitic recrystallization even at very low cooling rates. The sample was also subjected to a constant compressive force during the experiments which ensured that the sensor maintained good contact with the sample even if the sample hardens. During the experiments the dielectric cell was protected against the room atmosphere and a dried airflow minimized hydration of the sample. A nitrogen cooling device provided testing capability from 120 to 700 K. In isothermal processes the temperature was controlled to within 0.01 K.

Nuclear Magnetic Resonance (NMR). ¹H NMR experiments were performed on a Bruker ASX spectrometer operating at 100 MHz. The spin–lattice relaxation time, T_{1z} , was measured with the inversion recovery pulse sequence ($\pi, \tau, (\pi/2), D_0$)_n typically using 16–18 values of τ and a recycle delay $D_0 > 5T_{1z}$. Typical inversion pulse lengths were 1.7 μ s. The rotating frame spin–lattice relaxation time $T_{1\rho}$ was determined by locking the signal after a $\pi/2$ pulse with a $\pi/2$ phase-shifted field pulse and observing subsequent signal intensity as a function of the field pulse duration. In all the studied temperature range, rapid spin diffusion results in an exponential decay of the magnetization which allows us to define a single relaxation rate. The sample used in NMR experiments was sealed under vacuum in glass tubes and the temperature was varied between 100 and 410 K, controlled by a conventional gas flow system, to within ± 1 K.

Identification of the solid state forms of indomethacin was performed by solid state ¹³C NMR. The ¹³C spectra were recorded at room temperature on a Bruker AV400 solid-state NMR spectrometer operating at 100.61 MHz by using a

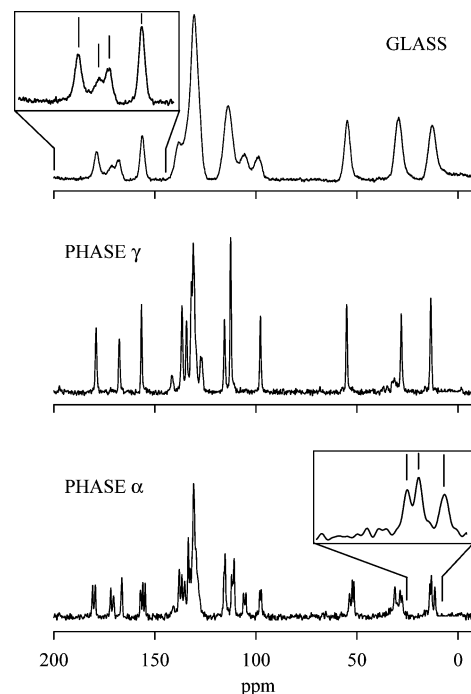


Figure 2. ¹³C NMR spectra of the glassy and crystalline γ - and α -phases recorded at room temperature.

Hartmann–Hann cross-polarization pulse sequence and proton decoupling during FID acquisition. The spectra were acquired with 8K data points using a dwell time of 10 μ s, and averaged with a number of acquisitions necessary to obtain a good resolution (256–4096). The chemical shifts were indexed from tetramethylsilane used as a standard reference. According to room temperature ¹H relaxation measurements, a recycle delay of 60s was used in order to ensure a complete relaxation of all protons in the samples. All samples were spun at the magic angle at 10 kHz in a 4 mm standard CPMAS NMR probe.

The spectra of the glass and crystalline phases (α , γ) are presented in Figure 2. The ¹³C chemical shifts of the γ -phase are in good agreement with those measured in a DMSO-*d*₆ solution and with previous solid-state investigations.^{16–18} The difference between the γ - and α -phase spectra lies, for the α -phase, in the presence of additional resonances at 105–106 and 170–172 ppm. Moreover a splitting of several resonance lines, clear seen for the chemical shift lower than 60 ppm, is observed. This splitting gives rise to a triplet which may be related to the existence of three different molecular conformations in agreement with the crystalline structure.¹⁴ The spectrum of the amorphous state is also represented in Figure 2. This spectrum gives chemical shifts that are similar to those measured in the α -phase with a broadening of the resonance lines due to the wide range of environment for the carbon atoms resulting from the lack of long range order.

III. Results

III.1. The Amorphous Form. Isothermal Dielectric Experiments: Above T_g . We have measured the real $\epsilon'(\omega)$ and imaginary $\epsilon''(\omega)$ part of the complex dielectric response $\epsilon^*(\omega) = \epsilon'(\omega) - i\epsilon''(\omega)$ as a function of temperature, between 363 and 315 K. As a characteristic and well-known feature of supercooled liquids, an asymmetrical broadening of the dielectric loss $\epsilon''(\omega)$ with respect to the simple Debye behavior is observed. The underlying dispersion of relaxation times can numerically be well accounted for by using the empirical formula given by Havriliak–Negami:

$$\epsilon^*(\omega) = \epsilon_\infty + \frac{\Delta\epsilon}{(1 + (i\omega\tau_{\text{HN}})^\alpha)^\beta} \quad (1)$$

where τ_{HN} denotes a characteristic relaxation time, ϵ_∞ , ϵ_s , and $\Delta\epsilon = (\epsilon_s - \epsilon_\infty)$ are the dielectric constant in the high-frequency limit, the static permittivity and the dielectric relaxation strength, respectively. The exponents α and β within the limit $0 \leq \alpha, \beta \leq 1$ introduce a symmetric and asymmetric broadening of ϵ'' -($\log \omega$) if values below 1 are chosen ($\alpha = \beta = 1$ corresponds to a Debye process exhibiting the characteristic full width at half-maximum of 1.14 decades). As a representative result for the measurements and fits, we present a selection of real $\epsilon'(\omega)$ and imaginary parts $\epsilon''(\omega)$ of the dielectric constant in Figure 3. For all the temperatures, we derived from the $\epsilon'(\omega)$ and $\epsilon''(\omega)$ data the parameters τ_{HN} , $\Delta\epsilon$, α , and β as a function of temperature. The α and β exponents keep a nearly constant value on the probed temperature range ($\alpha \approx 0.85$; $\beta \approx 0.58$); ϵ_s increases and ϵ_∞ decreases as the temperature decreases according to the following expression:

$$\epsilon_i(T) = A_i + \frac{B_i}{T} \quad (i = s, \infty) \quad (2)$$

with $A_s = 5.705$, $B_s = 875$ K, $A_\infty = 0.983$ and $B_\infty = -1738$ K. The temperature dependence of the fit parameters α , β , ϵ_s , and ϵ_∞ are reported in Figure 4. As predicted by the Onsager theory, $\Delta\epsilon$ is proportional to $1/T$. The refractive index can be deduced from ϵ_∞ using the relation: $n = \sqrt{\epsilon_\infty/1.05}$, where the constant 1.05 is an average value introduced for nonpolar liquids to take into account the atomic polarization.¹⁹

The temperature evolution of the relaxation times τ_{HN} resulting from the refinement is displayed in the Arrhenius plot in Figure 5 (open circles). The rate of the primary relaxation follows the VFT equation:

$$\tau(T) = \tau_0 \exp\left(\frac{DT_0}{T - T_0}\right) \quad (3)$$

with $\tau_0 = 2.6 \times 10^{-20}$ s, $T_0 = 230.5$ K, and $D = 18.5$. The dimensionless parameter D , called strength parameter, is related to the steepness index m :²⁰

$$m = \left(\frac{D}{\ln 10}\right) \left(\frac{T_0}{T_g}\right) \left(\frac{1}{1 - T_0/T_g}\right)^2 \quad (4)$$

Here T_g is the glass transition temperature corresponding to a relaxation time $\tau = 100$ s. From the above VFT parameters, we obtained $T_g = 316$ K and a steepness index $m = 79$, which is identical to the value determined from the temperature modulated DSC measurements.²¹

Isochronal Dielectric Experiments: Sub- T_g . A preliminary slow cooling rate experiment ($q = 1$ K/min) has been performed between $T = 350$ K and $T = 173$ K at 6 frequencies (1 Hz, 10 Hz, 100 Hz, 1 kHz, 10 kHz, 100 kHz) in order to localize the position of sub- T_g β relaxations. The term “ β process” is used at once to designate motions of only a part of a molecule or the so-called Johari–Goldstein β -relaxation (JG). In the present case, except a well-defined relaxation peak associated with the α -process observed above T_g , below T_g the $\epsilon''(T)$ thermograms did not show any dynamic process in the explored temperature/frequency range. Nevertheless, it has been shown in some compounds that the thermal history can affect the amplitude of the β process.²² In this case, the authors suggest that, in view of the β -relaxation instability, it is possible to observe a

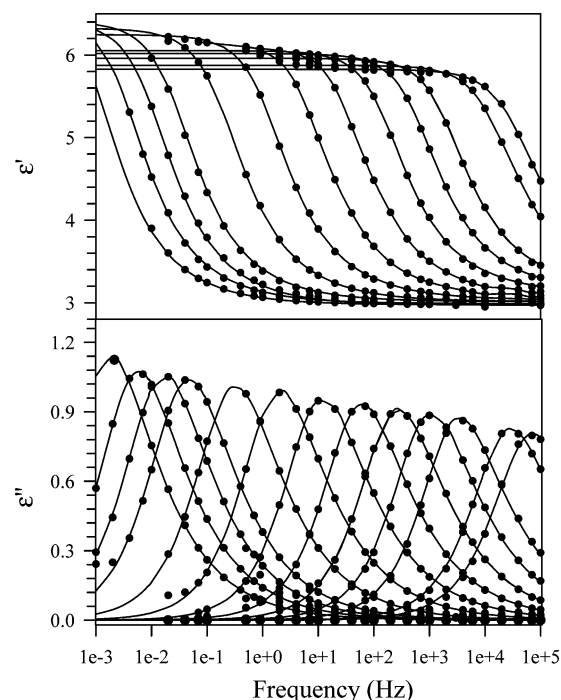


Figure 3. Real and imaginary parts of the dielectric susceptibility of amorphous indomethacin at various temperatures: the lowest temperature curve was recorded at the calorimetric glass transition temperature 315 K, the other curves refer to temperatures 317–363 K in the order of increasing peak frequency. The solid lines result from fits with the Havriliak–Negami function.

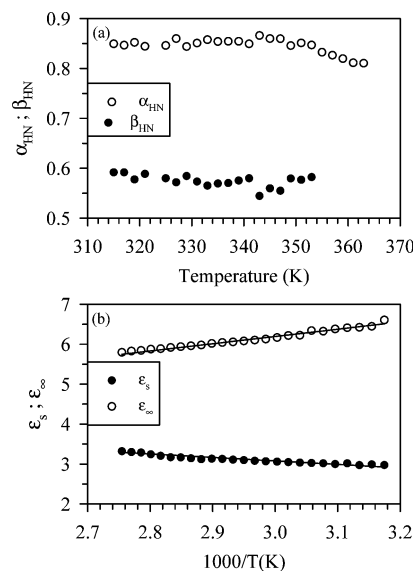


Figure 4. (a) Asymmetric β_{HN} and symmetric α_{HN} broadening parameters of the Havriliak–Negami relaxation function as a function of temperature (at high temperature, the high-frequency size of the loss factor is not determined thus preventing a precise determination of the β_{HN} parameter). (b) Static permittivity ϵ_s (full circles) and high-frequency permittivity ϵ_∞ (open circles) as a function of the reciprocal temperature.

β -process after a rapid quench of the liquid. To perform the fastest deep quench, indomethacin has been melted on the dielectric cell and placed in the analyzer previously cooled at $T = 170$ K. The dielectric susceptibility $\epsilon^*(T)$ has been determined upon heating at $q = 1$ K/min to 300 K. Figure 6 shows the temperature evolution of the loss factor $\epsilon''(T)$ obtained for four of the eight studied frequencies [3 Hz, 10 Hz, 30 Hz, 100 Hz, 300 Hz, 1 kHz, 3 kHz, 10 kHz]. Contrary to the slow

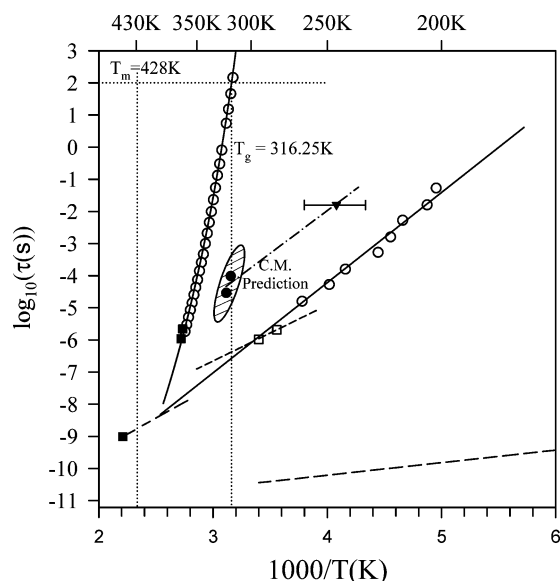


Figure 5. Relaxation map of indomethacin: The open circles refer to the relaxation time determined by dielectric measurements: isothermally above T_g and fitted with the Havriliak–Negami function; isochronally below T_g and determined from the temperature of the maximum loss factor below T_g . The solid lines represent the VFT (α -process) and Arrhenius (sub- T_g process) resulting refinements. The closed circles correspond to the relaxation times predicted by the coupling model and determined from relation 6, the low temperature point (\blacktriangledown) is obtained from isochronal dielectric loss factor of the deeply quenched liquid. The full squares correspond to the ^1H NMR T_{1z} (short times) and $T_{1\rho}$ (long time) minima of the amorphous, the open squares to the $T_{1\rho}$ minima measured in the crystalline γ -phase. The dashed lines result from refinements of the NMR relaxation times using the model and the parameters (Table 3) described in the text.

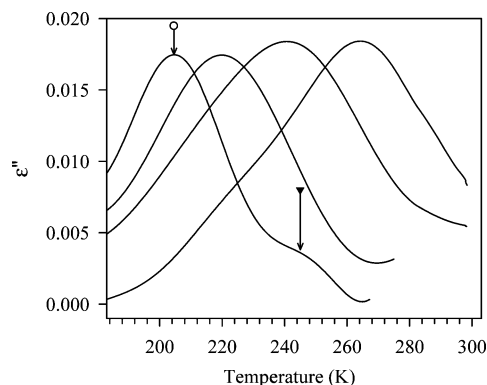


Figure 6. Isochronal dielectric loss factor measured, after a rapid and deep quench below T_g , while scanning the temperature upon heating at $q = 1$ K/min. Data are shown for frequencies 10 Hz, 100 Hz, 1 kHz, and 10 kHz in order of increasing temperature. At 10 Hz, the vertical arrows point the location of the temperature of the maximum loss factor corresponding to intramolecular contributions (\circ) and to the Johari–Goldstein process (\blacktriangledown).

cooling rate experiment, the loss factors are characterized by a broad and low amplitude relaxation peak resulting from the existence of residual molecular mobility in the glassy state. The relaxation time, defined as $\tau_{\max} = (2\pi\nu_{\max})^{-1}$, is reported as a function of the reciprocal of the loss peak temperature in the Arrhenius plot Figure 5. The temperature evolution of the relaxation times follows the Arrhenius equation:

$$\tau(T) = \tau_0 \exp\left(\frac{E}{RT}\right) \quad (5)$$

$$\tau_0 = 9.5 \times 10^{-17} \text{ s and } E_\beta = 56 \text{ kJ/mol}^{-1}.$$

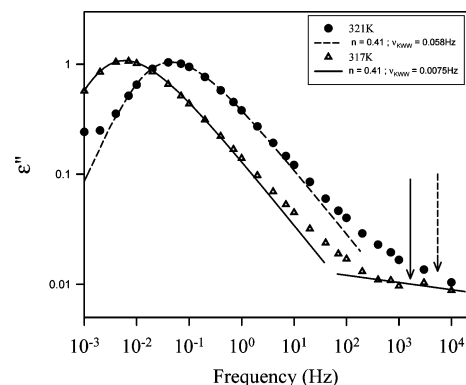


Figure 7. Dielectric loss of indomethacin at 317 and 321 K. The lines are KWW fits to the α -relaxation peaks with $n = 0.41$. The vertical arrows point the location of the relaxation frequency calculated from relation 6.

As we can see in Figure 6, the 10 Hz data shows not only a loss peak but a shoulder at higher temperatures indicating the presence of a possible slower secondary relaxation. Partially hidden under the predominating low temperature peak, only a crude estimation of the temperature of this relaxation is possible. The corresponding point is reported in Figure 5. As a test to determine the origin of these relaxations we have used the relation developed in the framework of the coupling model.²³ This model establishes a relation between the α -relaxation times and a primitive relaxation time τ_0 which is expected to be comparable to the τ_β of the JG relaxation:²⁴

$$\tau_0 = (t_c)^n (\tau_\alpha)^{(1-n)} \quad (6)$$

where n is the coupling parameter and t_c a characteristic time having the approximate value of 2×10^{-12} s for small molecular liquids. The result of a refinement using the Fourier transform of the Kohlrausch–Williams–Watt function $\varphi(t) \propto \exp(-(t/\tau_\alpha)^{\beta_{\text{KWW}}})$ (with $\beta_{\text{KWW}} = 1 - n$), for the two lowest investigated temperatures, is reported in the log–log representation of ϵ'' in Figure 7. The two corresponding values of τ_0 are reported in Figure 5 in the dashed zone and are clearly distinct from the low temperature process but can reasonably be connected to the high-temperature relaxation, making of this process the genuine Johari–Goldstein β -relaxation. To get more insight concerning the origin of these processes, ^1H NMR experiments were performed.

NMR Analysis. The temperature dependence of the proton spin–lattice relaxation times T_{1z} (full circles) $T_{1\rho}$ (full and open squares), and the spin–spin relaxation time T_2 (full triangles), determined from the full width at half-maximum (fwhm) of the NMR spectral line, of amorphous indomethacin are reported in Figure 8.

It is well-known that the line shapes and relaxation times in ^1H NMR experiments are sensitive to structural and motional parameters. The ^1H transversal relaxation time T_2 , which is related to the inverse NMR line width, can provide qualitative information about the solid-state molecular motions since an increase of molecular mobility leads to a narrowing of the NMR absorption line. These properties are useful for investigating the polymorphism of materials. As we can see in the inset of Figure 8, in the glassy state ($T < T_g$), the NMR spectrum is broad and T_2 keeps approximately a constant rigid value of 10 μs . In the metastable state ($T > T_g$), the increase of molecular mobility induces a motional line narrowing and a variation of T_2 . According to the Arrhenius diagram of Figure 5, the motional

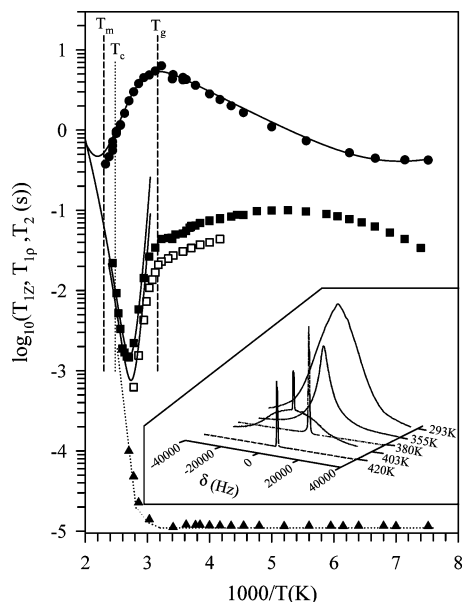


Figure 8. Representation of proton T_{1z} (●), $T_{1\rho}$ (■, $B_1 = 18$ G; □, $B_1 = 10$ G), and T_2 (▲) relaxation times of amorphous indomethacin as a function of the reciprocal temperature. The full lines correspond to the model and parameters described in the text. The dotted lines are only a guide for the eyes. Inset: temperature evolution of the ^1H NMR spectra from the glassy to the liquid state. At $T_c = 403$ K, the very broad contribution under the narrow peak of the metastable liquid corresponds to the crystallization of indomethacin toward the α -phase.

process responsible for this line narrowing corresponds to the cooperative motion observed by dielectric relaxation. As the temperature is increased, molecular motion becomes fast enough to average an important part of the dipolar interactions responsible for the broad NMR spectral lines observed below T_g . As a result a sharp “liquid-like” spectrum constituted of three lines is seen at $T \approx 380$ K. At $T \approx 403$ K, the metastable state begins to crystallize. The corresponding two phases NMR spectrum is composed by a broad solidlike pattern superimposed with a sharp liquidlike component. The broad component of the spectrum disappears around 420 K which indicates that the crystallization occurred toward the α -phase.

To extract the motional parameters from the temperature evolutions of the spin–lattice relaxation times T_{1z} and $T_{1\rho}$ we have used the standard relations (BPP model):²⁵

$$\frac{1}{T_{1z}} = C[J(\omega_0, \tau) + 4J(2\omega_0, \tau)] \quad (7)$$

$$\frac{1}{T_{1\rho}} = C\left[\frac{3}{2}J(2\omega_1, \tau) + \frac{5}{2}J(\omega_0, \tau) + J(2\omega_0, \tau)\right] \quad (8)$$

Here C is a relaxation constant expressed as the part of the second moment averaged by the considered motion:

$$C = \frac{2}{3}\gamma_H^2 \Delta M_2 \quad (9)$$

In the case of a single-exponential relaxation, the spectral density $J(\omega_i, \tau)$ is given by the following:

$$J(\omega_i, \tau) = \frac{\tau}{1 + (\omega_i \tau)^2}; \quad \omega_i = \gamma_H B_i \quad (i = 0, 1) \quad (10)$$

γ_H is the proton nuclear gyromagnetic ratio. In the frame of a BPP model, it is well established that the relaxation rates exhibit a minimum when the correlation time τ follows the relations

$$\omega_0 \tau = 0.616(T_{1z}) \quad (11)$$

$$\omega_1 \tau = 0.5(T_{1\rho}) \quad (12)$$

As seen in Figure 8, T_{1z} exhibits a minimum in the glassy state at $T = 140$ K. The occurrence of a second minimum is expected at high temperature, just above T_m . Below T_g , a good description of the temperature dependence of T_{1z} is obtained using the BPP model (eq 7) and an Arrhenius evolution of the correlation times (eq 5). The best refinement gives the following parameters: $\tau_0 = 1.7 \times 10^{-12}$ s and $E_a = 7.85$ kJ/mol. As generally observed in similar compounds, this T_{1z} minimum is ascribed to the C3 rotation of the methyl group for which an activation energy value E_a lying in the range 7–10 kJ/mol is generally observed.^{26–29} Moreover, as for other molecules where the relaxation arises from methyl rotation, and if we suppose that all other protons are relaxed by rapid exchange to and from methyls groups, the constant C (eq 9) is given by ref 26:

$$C = \frac{9}{20} \frac{n}{N} \frac{\gamma^4 \hbar^2}{b^6} \quad (13)$$

Here N is the total number of protons of the molecule, n is the number of protons in the methyl groups contributing to the relaxation process, and b is the interproton distance in methyl groups. For indomethacin, assuming that a single methyl group contribute to the relaxation ($n = 3$, $N = 16$) and using the value of Table 3, we obtained (eq 13) $b = 1.88$ Å, which is close to the value of 1.8 Å generally observed. This result supports our model of relaxation mechanism and supposes the existence of a second minimum ascribed to the second methyl group at lowest temperature. Above T_g , the T_{1z} relaxation curve is also well described using the BPP model (eq 7) with $E_a = 37.7$ kJ/mol and $\tau_0 = 4.4 \times 10^{-14}$ s. From these results the occurrence of a T_{1z} minimum is expected just above T_m . Upon increasing the temperature, the crystallization in the α -phase is responsible for the deviation from the BPP model observed around $T = T_c$. However, the crystallization is not complete since T_{1z} is significantly lower than that corresponding to the α -phase (Figure 9). Thus, the T_{1z} measured above T_c does not correspond to a stable state.

In the metastable domain, $T_{1\rho}$ exhibits a minimum at $T = 295$ K. From eq 12 and the report of the corresponding correlation times measured at the minimum in the Arrhenius diagram (Figure 5), we conclude that $T_{1\rho}$ is monitored by the α -process revealed in dielectric spectroscopy. An attempt to fit the experimental data with a BPP model assuming an Arrhenius activation law (eq 5) gives unphysical parameters. This result could be related to the amorphous nature of this phase. It is well-known that in glass-forming liquids the existence of different environments often results in a non-Debye relaxation which cannot be described by the BPP model using a single correlation time τ . For indomethacin, this property is clearly demonstrated by the dielectric parameters values α_{HN} and β_{HN} (cf. Figure 4). To compare the dielectric and NMR residence times, we have introduced a correlation time distribution for the description of the temperature dependence of $T_{1\rho}$. Among various phenomenological distributions, a Cole–Cole distribution was used in order to take into account the almost symmetric shape of the $T_{1\rho}$ temperature dependence.

TABLE 3: Activation Energy E , Preexponential Factor τ_0 , and Second Moment M_2 Obtained from the NMR Analysis of the Relaxation Curves Using the Model Described in the Text

	$T_{1z}(\text{HT})$	$T_{1z}(\text{LT})$	$T_{1\rho}(\text{HT})$ (VFT)	$T_{1\rho}(\text{LT})$ γ -phase	T_{1z}	
					α -phase	γ -phase
E (kJ/mol)	37.7	7.8	35.5	33.3	10.4	10.4
τ_0 (s)	4.4×10^{-14}	1.7×10^{-12}	2.6×10^{-20}	1.3×10^{-12}	0.41×10^{-12}	0.41×10^{-12}
M_2 (G ²)	1.93	2.26	4	0.09	3.37	2.26

In this case, the spectral density is given by ref 30:³⁰

$$J(\omega) = \frac{1}{\omega} \sin\left(\alpha_{\text{CC}} \frac{\pi}{2}\right) \left[\frac{(\omega\tau)^{\alpha_{\text{CC}}}}{1 + (\omega\tau)^{2\alpha_{\text{CC}}} + 2 \cos\left(\alpha_{\text{CC}} \frac{\pi}{2}\right) (\omega\tau)^{\alpha_{\text{CC}}}} \right] \quad (14)$$

A good description of the experimental data was obtained using this distribution law in association with the Vogel–Fulcher–Tamman expression of the correlation times deduced from the dielectric data (Table 3). The broadening coefficient $\alpha_{\text{CC}} = 0.5$ confirms the existence of a large correlation times distribution. As shown in Figure 8, below T_g this model completely fails to describe the temperature dependence of $T_{1\rho}$ and the relaxation is no longer governed by the cooperative α -relaxation process.

All these results are gathered together in Table 3 and are plotted as filled squares (for the position of the different minimum) and dashed lines (for the fit parameters) along with the dielectric data on the Arrhenius diagram of Figure 5.

III.2. The Crystalline Phases. Dielectric investigations of the crystal forms of indomethacin were performed between 150 and 470 K, but no variation of the dielectric susceptibility was observed. It indicates that either no motion exists in these phases either if it exists, it does not involve a change of orientation of the associated dipole. In this case, the NMR method remains applicable and relaxation rates measurements still offers an interesting method to get insight on the molecular dynamics. The temperature dependence of the proton spin–lattice relaxation times T_{1z} (full circles), $T_{1\rho}$ (full and open squares), and the spin–spin relaxation time T_2 (full triangles) measured in the crystalline phases are reported in Figure 9. Contrary to the

glassy state, T_2 displays a constant value in the whole investigated temperature domain, indicating that the release of the motion observed above T_g does not exist in the crystalline phases. For both forms, T_{1z} exhibits a low-temperature minimum at $T \approx 162$ K, which is associated, by comparison with the previous analysis of the glassy state, to a C3 rotation of a methyl group. For the γ -phase (Figure 9), the extension to 105 K of the T_{1z} measurements indicates the occurrence of a second minimum at lower temperature ($T < 100$ K). The existence of this minimum, associated with the second methyl group motion, confirms our interpretation of the T_{1z} curve in the glassy state.

Assuming that this motion follows an Arrhenius thermally activated process, a good description of the experimental data was obtained using the BPP model, with the same parameters for the two crystalline forms: $\tau_0 = 0.41 \times 10^{-12}$ s and $E_a = 10.4$ kJ/mol. Again, the E_a value corresponds to a methyl rotation, which appears here more hindered in the crystals than in the amorphous state. The small difference between the C constants of the γ -phase (which is identical to those measured in the glass) and the α -phase (cf. Table 3) indicates the existence of a more important steric hindrance in the α -phase. It results in a more important intermolecular contribution, leading to an increase of M_2 to 3.37 G².

In the crystalline phases, an important difference of behavior is observed in the temperature evolution of $T_{1\rho}$. As seen in Figure 9, in the high-temperature region, a $T_{1\rho}$ minimum is only perceived for the γ -phase ($T = 317$ K; $B_1 = 9$ G and $T = 325$ K; $B_1 = 17$ G). We have obtained a reasonable match of the experimental data by using the BPP model with the parameters of Table 3. Below $T \approx 250$ K, the rotating frame relaxation is monitored by the relaxation mechanism observed by T_{1z} i.e., methyl C3 rotation. However the temperature dependence of $T_{1\rho}$ does not follow the usual BPP relation: $T_{1\rho} = T_{1z}$ for $\omega\tau \ll 1$. As a consequence, the calculation of $T_{1\rho}$ with the parameters deduced from T_{1z} analysis, represented as a solid line in Figure 9, gives only a qualitative description of the experimental data. This result is probably due to the additional contribution coming from the second methyl rotation which is not taken into account in our model.

IV. Discussion

Dynamic Properties of the Metastable Supercooled Liquid.

The results have to be discussed referring to the typical frequency dependence of the dielectric susceptibility in glass forming materials which is characterized by the following sequence of dynamic processes. Near T_g , the α -relaxation presents a peak located at rather low frequencies, whose freezing marks the glass transition. Some decades above, a β -peak of lower amplitude is associated with a relaxation process inherent to glass formers. In some cases, this β -peak is only perceivable in the flank of the predominating α -peak by its high-frequency tail, so-called “excess wing” whose assimilation to the slow β -process is now commonly admitted. At higher frequency, the loss factor can be approximately described by a $\nu^{-\lambda}$ dependence. The small positive exponent λ reflects the very slow frequency variation of this dispersion which is thus called the “nearly constant loss” (NCL).

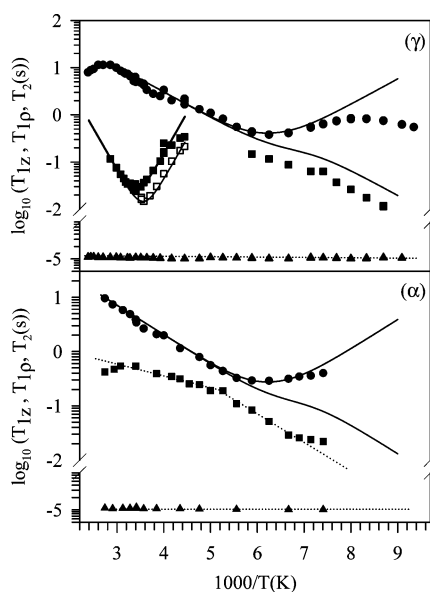


Figure 9. Representation of proton T_{1z} (●), $T_{1\rho}$ (■, $B_1 = 17$ G; □, $B_1 = 9$ G), and T_2 (▲) relaxation times of the crystalline γ -phase and α -phase of indomethacin as a function of the reciprocal temperature. The full lines correspond to the models and parameters describe in the text. The dotted lines are only a guide for the eyes.

A marked feature of the dynamic properties of indomethacin concerns the temperature evolution of the α -relaxation times. Some characteristics are conformable to the general trend observed in glass-forming systems: at the calorimetric glass transition, the primary relaxation time τ reaches the value of 100s. Moreover, the steepness index $m = 79$ and the fractional exponent $\beta_{\text{KWW}}(T_g) = 0.59$ determined from the refinements (cf. section III) are in good agreement with the phenomenological relation establishing correlations between the fragility and the nonexponential character of the structural relaxations.²⁰ However, while the low-frequency NMR and dielectric relaxation times follow a VFT evolution, the continuity with the high-frequency NMR data determined from the $T_{1\rho}$ cannot be understood without a change of the dynamic behavior in the high temperature domain. The very low value of the pre-exponent factor $\tau_0 = 2.6 \times 10^{-20}$ s supports the necessity to consider more than one dynamic regime to describe the overall temperature evolution of the relaxation times. The present refinement parameters of the VFT relation ($T_0 = 230.5$ K, $D = 18.5$) are different from those published in ref 7 ($T_0 = 263.7$ K, $D = 7.29$) but are in reasonable agreement with those published in ref 32 ($T_0 = 233$ K, $D = 14.4$). The comparison with viscosity data reveals an atypical behavior in the temperature evolution of the related physical quantities. The VFT parameters of the temperature dependence of the viscosity ($T_0 = 256$ K, $D = 8.9$)^{3,32} give a value of $\eta = 4.5 \times 10^{10}$ Pa·s at T_g , whereas $\eta = 10^{12}$ Pa·s (which is associated with the relaxation time $\tau = 100$ s) is the traditionally expected value at the calorimetric glass transition temperature. This difference of nearly 2 orders of magnitude at T_g indicates the existence of a decoupling in the temperature evolution of the relaxation times and the transport coefficients. Decoupling of the dynamics has been mentioned several times, or can be assumed from the confrontation of experimental data obtained with different techniques. We can quote the examples of phenolphthalein, 1,3,5-tri- α -naphthylbenzene (TNB), meta-toluidine, triphenyl phosphite (TPP) (one of the more pronounced decoupling with $\eta(T_g) < 10^9$ P). Such differences show, on one hand that the determination of the steepness index m can be dependent on the experimental technique used, and on the other hand that an important residual mobility can exist just below T_g .

When a slow cooling below T_g is performed, there is no evidence of secondary relaxations, in particular the JG process, during isothermal and isochronal dielectric measurements, through a well-defined loss peak. This situation could correspond to a JG process largely hidden under the α -peak. In that case, the relaxation time τ_β associated with the JG process must be close to the primary relaxation time τ_α . This is usually observed for small $n = 1 - \beta_{\text{KWW}}$ values, which also seems to be correlated to a dielectric strength $\Delta\epsilon_\beta$ of low amplitude.³¹ The refinement of the low-frequency part (α contribution) of the dielectric loss with a KWW function gives values $n = 0.41$ for the two lowest temperatures peaks of Figure 7. The n value agrees with a secondary relaxation of low amplitude. After a rapid and deep quench of the liquid, the isochronal dielectric loss factor exhibits two sub T_g -relaxations, the lower temperature process being attributed to the JG process. As a consequence, the JG relaxation in indomethacin is difficult to observe, partly due to its low amplitude and its proximity to other processes (α -relaxation and local rotation), but also due to its sensitivity to aging.

The third dynamic process, the NCL regime, which is the high frequency contribution to the dynamic sequence in supercooled liquids, has recently received sustained attention.

The best candidates to study this regime are those glass-formers that have secondary relaxations processes of very low amplitude and a short separation with the α -process, which corresponds to a small n value. From this point of view, indomethacin satisfies particularly well to these criteria. In Figure 7, the slow variation of the loss factor at high frequency could be related to the NCL contribution reflecting some mobility which, in the coupling model approach, would result from short time caged dynamic of relaxing species.³³ Nevertheless, the presence of the JG relaxation in the same frequency domain as indicated by the vertical arrows in Figure 7 makes the analysis difficult.

The Crystalline Phases. The NMR study of the dynamic properties of indomethacin crystalline forms has revealed the existence of a relaxation process in the more stable γ -phase. This slow motion is observed in the temperature dependence of the spin-lattice relaxation time $T_{1\rho}$, by a pronounced and deep minimum. As we are in a temperature domain where the methyl group rotation is fast, the extreme narrowing condition is fulfilled for this motion and we should have observed $T_{1\rho} = T_{1\rho}$. Consequently methyl group rotation cannot be at the origin of this minimum. The examination of the molecule structure (Figure 1) allows us to suggest as a possible origin of this relaxation process: the rotation of the methoxy group around the C–O axis or the rotation of the chlorobenzyl group around the N–C axis. According to the structural analysis of the crystalline phases, the chlorobenzyl group dynamic is forbidden in the crystalline α -phase, partly due to the additional hydrogen bonds between the carboxylic acid and an amide carbonyl resulting from the organization of the molecules in trimers.¹⁴ We can then conclude that this motion is the one probed by $T_{1\rho}$ in the high-temperature range of the γ -phase. This hypothesis is consistent with the refined activation energy value which is on the same order of magnitude than that obtained for similar motions: $E_a = 42$ kJ/mol.^{26–28}

Origin of the Glassy State Relaxation Processes. After a rapid and deep quench of liquid indomethacin into the glassy state, the temperature evolution of the dielectric loss factor measured upon heating has revealed the existence of a dynamic process which seems to coincide with that of the γ -phase observed by NMR. Two arguments allow to show that this process has no relation with a JG-type relaxation: the use of coupling model, which generally well describes correlations with the α -process, localizes the JG-relaxation in a very different frequency/temperature domain; this secondary relaxation exists also in the crystalline γ -phase and is therefore not a JG relaxation according to the criteria given by ref 31. Indeed, when reported in the Arrhenius plot of the supercooled liquid (cf. Figure 5), the two $T_{1\rho}$ minima of the γ -phase perfectly superimposed to the Arrhenius law associated with the sub- T_g relaxation process of the rapidly quenched compound, whose corresponding activation energy, $E_a = 56$ kJ/mol, determined from low amplitude and very broad loss factors, is reasonably close to the activation energy of the γ -phase. This process has already been observed by thermally stimulated depolarization current (TSDC) experiments.¹⁰ In that case, the data have shown in the glassy state a secondary relaxation characterized by a very low intensity and a low activation energy (estimated energy distribution between 28 and 40 kJ/mol) and corresponding to very localized and low amplitude molecular motions. The existence of this process was also suggested from mechanical relaxation data.³

Our results provide fundamental information concerning the properties of glassy indomethacin. First, the glassy states obtained by a rapid quench and by a slow cooling are not

identical; an important residual mobility can be maintained after a rapid quench. This residual motion is similar in nature to that observed in the γ -phase. Second, the sub T_g contribution characterized from isothermal dielectric measurements on the slowly cooled metastable liquid, and the decoupling of the relaxation modes indicate the persistence of relaxation processes below T_g .

Influence of the Sub- T_g Relaxations on the Crystallization of Indomethacin. Some results indicated that crystallization of indomethacin is initiated in the glass transition region⁶ and that the crystalline form obtained upon heating depends on the thermal treatment (rapid or slow cooling). Observations of crystallization in the glass transition region have been reported on fragile glass-forming liquids.³⁴ It has been argued that the main process controlling the crystallization rate in these systems was the JG-relaxation. In indomethacin two scenarios can be considered to explain the initiating effects of the crystallization by the creation of crystal embryo in the glassy state. In the first case, the subsistence of non negligible molecular mobility can be attributed to diffusion processes due to the decoupling, close to T_g , of the viscosity with the dielectric relaxation times. In the second case the mobility far below T_g inducing the crystal nucleation comes from the combined effects of the Johari–Goldstein relaxation and the rotation of the chlorobenzyl group.

V. Conclusion

The combination of dielectric and NMR measurements has permitted to characterize the molecular mobility of indomethacin in its different forms. Below T_g , the observations can be summarized as follows:

- No dynamic exists in the α -phase, except methyl group rotations.
- The crystalline γ -phase is characterized by the existence of rotational dynamics related to the chlorobenzyl group motion, solely observed by NMR
- The existence of an important molecular mobility is seen in the rapidly and deeply quenched liquid. This motion is also present in the crystalline state (γ) which is incompatible with its assimilation to the Johari–Goldstein process. Referring to the γ -phase, it is attributed to the chlorobenzyl group rotation. The excess of mobility observed in that case²² makes the corresponding motion observable by dielectric relaxation.
- In the amorphous state, a trace of a Johari–Goldstein relaxation process is observed after a rapid quench. This mobility could favor the appearance, below T_g in the rapidly quenched liquid, of crystal embryo of the α -phase, the chlorobenzyl group rotation leading in that case to the formation of molecular bonds between a carboxylic acid group and an amide carbonyl group. This local ordering would then be the precursor of the organization of the molecules in trimers, giving rise to the crystallization of the sample toward the α -phase upon heating. The diffusion observed around T_g would favor an ordering of the molecule in dimers to allow the crystallization toward the

more stable γ -phase. Structural investigations of the supercooled liquid and of the glassy state are under way to detect the temperature dependence of the local ordering of the molecules in dimers or trimers. A more precise characterization of the Johari–Goldstein relaxation is also a perspective.

Acknowledgment. We gratefully acknowledge the financial support by the FEDER in the frame of an interreg III program (Nord-Pas de Calais, Haute Normandie, Kent).

References and Notes

- (1) Hancock, B. C.; Zografi, G. *J. Pharm. Sci.* **1997**, *86*, 1.
- (2) Craig, D. Q. M.; Royal, P.; Kett, V.; Hopton, M. *Int. J. Pharm.* **1999**, *179*, 179.
- (3) Andronis, V.; Zografi, G. *Pharm. Res.* **1997**, *14*, 410.
- (4) Plazek, D. J.; Magill, J. H. *J. Chem. Phys.* **1966**, *45*, 3038.
- (5) Yoshioka, M.; Hancock, B. C.; Zografi, G. *J. Pharm. Sci.* **1994**, *83*, 1700.
- (6) Andronis, V.; Zografi, G. *J. Non-Cryst. Solids* **2000**, *271*, 236.
- (7) He, R.; Craig, D. Q. M. *J. Pharm. Pharmacol.* **2001**, *53*, 41.
- (8) Hancock, B. C.; Dupuis, Y.; Thibert, R. *Pharm. Res.* **1999**, *16*, 672.
- (9) Hancock, B. C.; Shamblin, S. L. *Thermochim. Acta* **2001**, *380*, 95.
- (10) Correia, N. T.; Moura Ramos, J. J.; Descamps, M.; Collins, G. *Pharm. Res.* **2001**, *18*, 1767.
- (11) Borka, L. *Acta Pharm. Suecica* **1974**, *11*, 295.
- (12) Fukuoka, E.; Makita, M.; Yamamura, S. *Chem. Pharm. Bull.* **1986**, *34*, 4314.
- (13) Kistenmacher, T. J.; Marsh, R. E. *J. Am. Chem. Soc.* **1972**, *94*, 1340.
- (14) Chen, X.; Morris, K. R.; Griesser, U. J.; Byrn, S. R.; Stowell, J. G. *J. Am. Chem. Soc.* **2002**, *124*, 15012.
- (15) Kaneniwa, N.; Otsuka, M.; Hayashi, T. *Chem. Pharm. Bull.* **1985**, *33*, 3447.
- (16) Singh, S. P.; Parmar, S. S.; Stenberg, V. I.; Farnum, S. A. *J. Heterocycl. Chem.* **1978**, *15*, 13.
- (17) Wulff, M.; Alden, M.; Tegenfeldt, J. *Bioconjugate Chem.* **2002**, *13*, 240.
- (18) Apperley, D. C.; Forster, A. H.; Fournier, R.; Harris, R. K.; Hodgkinson, P.; Lancaster, R. W.; Rades, T. *Magn. Reson. Chem.*, in press.
- (19) Böttcher, C. J. F. *Theory of Electric Polarization*, 2nd ed.; Elsevier: Amsterdam, 1973; Vol. 1.
- (20) Böhmer, R.; Ngai, K. L.; Angell, C. A.; Plazek, D. J. *J. Chem. Phys.* **1993**, *99*, 4201.
- (21) Carpentier, L.; Bourgeois, L.; Descamps, M. *J. Therm. Anal. Cal.* **2002**, *68*, 727.
- (22) Wagner, H.; Richert, R. *J. Phys. Chem. B* **1999**, *103*, 4071.
- (23) Ngai, K. L. *J. Chem. Phys.* **1998**, *109*, 6982.
- (24) Ngai, K. L.; Lunkenheimer, P.; Leon, C.; Schneider, U.; Brand, R.; Loidl, A. *J. Chem. Phys.* **2001**, *115*, 1405.
- (25) Bloembergen, N.; Purcell, E. M.; Pound, R. V. *Phys. Rev.* **1948**, *73*, 679.
- (26) Andrew, E. R.; Glowinski, S. *Solid State NMR* **2000**, *18*, 89.
- (27) Andrew, E. R.; Kempka, M. *Solid State NMR* **1995**, *4*, 249.
- (28) Andrew, E. R.; Kempka, M.; Radomski, J. M.; Szczesniak, E. *Solid State NMR* **1999**, *14*, 91.
- (29) Van Putte, K.; Skoda, W.; Petroni, M. *Chem. Phys. Lipids* **1968**, *2*, 361.
- (30) Beckmann, P. A. *Phys. Rep.* **1988**, *171*, 85.
- (31) Ngai, K. L.; Paluch, M. *J. Chem. Phys.* **2004**, *120*, 857.
- (32) Andronis, V.; Zografi, G. *Pharm. Res.* **1998**, *15*, 835.
- (33) Ngai, K. L. *J. Phys.: Condens. Matter* **2003**, *15*, S1107.
- (34) Okamoto, N.; Oguni, M.; Sagawa, Y. *J. Phys.: Condens. Matter* **1997**, *9*, 9187.